

## RESEARCH ARTICLE

# On Practical RIS-Aided OFDM With Index Modulation

ELVAN KUZUCU HIDIR<sup>1</sup>, ERTUGRUL BASAR<sup>2</sup>, (Fellow, IEEE),  
AND HAKAN ALI CIRPAN<sup>1</sup>, (Senior Member, IEEE)

<sup>1</sup>Faculty of Electrical and Electronics Engineering, Istanbul Technical University, Maslak, 34469 Istanbul, Türkiye

<sup>2</sup>Communications Research and Innovation Laboratory (CoreLab), Department of Electrical and Electronics Engineering, Koç University, Sariyer, 34450 Istanbul, Türkiye

Corresponding author: Elvan Kuzucu Hidir (ehidir@itu.edu.tr)

This work was supported by TUBITAK under Grant 120E401.

**ABSTRACT** Reconfigurable intelligent surface (RIS)-aided communication has been regarded as one of the promising technologies for future wireless networks with regards to controlling the propagation environment and enhancing the quality of the end-to-end communication links. In this study, considering the importance of index modulation (IM) and RIS-aided schemes in 6G networks, first, an RIS-aided orthogonal frequency division multiplexing (OFDM)-IM system design is proposed. Previous studies focusing on RIS-aided OFDM systems are based on an ideal reflection model, where the constant amplitude and variable phase shift of the RIS are independent of the frequency of the incoming signal. However, in realistic applications, this ideal RIS model may not be accurate since both the phase shift and amplitude of RIS elements depend on the frequency, which makes their effect significant, especially for wideband systems. Therefore, this study primarily considers a practical RIS model through designing the RIS reflection coefficients for OFDM-IM systems. In order to further enhance the bit error rate (BER) performance of the RIS-aided OFDM-IM system, an exhaustive search-based optimization algorithm that maximizes the average minimum Euclidean distance (AMED) within the subblocks is also proposed. Moreover, extensive computer simulation results are produced in order to illustrate the performance improvement of the proposed algorithm over the reference algorithms in the literature. The proposed AMED-based reflection coefficient design algorithm provides better BER performance for RIS-aided OFDM-IM systems concerning the presented algorithms.

**INDEX TERMS** 6G, orthogonal frequency division multiplexing (OFDM), index modulation (IM), OFDM-IM, reconfigurable intelligent surface (RIS).

## I. INTRODUCTION

Reconfigurable intelligent surface (RIS)-aided communication systems have been considered as promising technologies for beyond fifth generation (5G) wireless communication. RIS-aided systems differ from traditional beamforming, amplify-and-forward (AF) relaying and MIMO schemes in terms of comprising several small, passive and low-cost elements that reflect/modify the impinging signals by adjusting proper phase shifts [1]. Since RIS elements do not require additional energy sources for the processing of radio frequency (RF) signals, encoding, decoding and hardware efficiency, RISs have been widely investigated for

existing wireless communication systems [2]. This makes RIS a revolutionary technology for the next-generation wireless systems [3], [4].

In recent years, to improve the performance of numerous RIS-aided wireless communication systems through adjusting RIS elements, novel RIS-aided designs are presented under different metrics that maximize energy efficiency (EE) [5], average sum-rate [6], [7], spectral efficiency (SE) [8], etc. for both single-user/multi-user systems [5], [6], [7], [8], [9], [10]. In these studies, the RIS design procedure generally focuses on joint optimization of transmit beamforming and power allocation.

It is worth mentioning that in the above studies, the considered RIS-aided communication systems mainly operate over frequency flat (non-selective) fading channels for

The associate editor coordinating the review of this manuscript and approving it for publication was Barbara Masini<sup>1</sup>.

narrowband communication systems. However, when frequency selective channels are considered for wideband communication systems, the optimization of the RIS reflection coefficients for all subcarriers, becomes more challenging. In the literature, there are limited works for RIS-aided wideband orthogonal frequency division multiplexing (OFDM) systems. A practical transmission protocol with channel estimation for the RIS-enhanced OFDM system is presented and passive RIS reflection coefficients are designed with estimated channel transmit power allocation by maximizing the achievable rate in [11] and [12]. RIS-enhanced wideband multiuser multiple-input single-output OFDM system is studied by designing both the RIS reflection coefficient and the transmit beamformer in order to maximize the achievable rate regarding whole subcarriers [13].

Although there are many studies on RIS-aided OFDM systems, the most of them assume an ideal RIS model, i.e., reflection coefficient of RIS element does not change with respect to different frequencies that means it has a variable phase shift and a constant amplitude independent from the frequency. However, this is impractical for realistic applications in wideband communication networks. In recent works, it has been demonstrated that there is always a fundamental relationship between the RIS reflection response, i.e., signal magnitude and phase shift, and the frequency of the incident wave where the signal exhibits different reflection coefficients with respect to the frequency [14], [15], [16]. However, especially for wideband communication systems, it has become a significant problem since the ideal reflection model cannot capture the correlation between these variables and can cause a noticeable performance loss in practical systems.

Recently, a novel concept called index modulation (IM) using the spatial domain in order to convey additional information with high energy and spectrum efficiency, has attracted considerable attention from academia and industry [17]. There are mainly two promising applications of the IM concept: spatial modulation (SM) and OFDM-IM, where the transmit antennas and subcarriers are used to convey information bits, respectively. In SM-based systems, information bits are transmitted through the conventional  $M$ -ary constellation symbols and the indices of the transmit antennas of a MIMO system [18]. Moreover, the IM concept can be effectively implemented for OFDM subcarriers inspired by SM. In the OFDM-IM scheme, information is conveyed both with  $M$ -ary symbols and with the indices of active subcarriers that are selected with respect to the incoming bits, while the remaining subcarriers are silent [19]. More recently, in order to improve the performances of both the OFDM-IM and the SM system, different schemes have been proposed that aim to maximize the MED of possible transmit vectors [20], [21], [22], [23], [24], [25], [26].

Regarding the aforementioned works that recognize the undeniable potential of both RIS and IM-aided wireless networks separately, we have examined the performance of

RIS-aided OFDM-IM communication systems, which has not been studied yet to the best of our knowledge. Moreover, the recent studies focus on RIS-aided OFDM systems that aim to optimize the reflection coefficients of RIS by maximizing the average achievable rate of the system; however, these works do not provide an optimal solution for RIS-aided OFDM-IM systems due to its empty subcarriers, which are different from OFDM. Therefore, in this study, we aim to design the reflection coefficient of RIS by considering the fundamental design criteria for OFDM-IM systems.

In this paper, firstly, we examine the fundamental relationship between the frequency and phase-amplitude of the incident signals from the RIS and introduce a novel system model for RIS-aided OFDM-IM systems by considering a practical RIS reflection model. Then, in order to design the reflection coefficients of RIS-aided OFDM-IM systems, we propose an exhaustive search-based algorithm that aims to maximize average minimum Euclidean distance (AMED) between the subblocks. Moreover, we provide extensive computer simulation results to illustrate the considerable BER performance improvement of the proposed algorithm over the reference systems utilizing RIS-aided OFDM. Furthermore, we obtain a significant BER performance enhancement with the considered practical model over the case of the ideal model.

The remaining of the paper is established as the following. We introduce the end-to-end system model of the RIS-aided OFDM-IM system by presenting the practical RIS model in Section II. In Section III, the proposed algorithm to design the reflection coefficient of RIS-aided system by considering the practical RIS model is presented. We exhibit numerical simulation results and investigate the BER performance of the system in Section IV and in Section V, we conclude our study.

## II. PRACTICAL RIS MODELING AND SYSTEM MODEL

In this section, firstly, we give a practical RIS model for wideband communication systems. Then, we present our system model for the RIS-aided OFDM-IM by considering the practical RIS reflection model.

### A. PRACTICAL RIS MODELING

The structure of RIS typically includes three layers and a smart controller. The outer layer comprises a significant number of metallic elements on a dielectric substrate that interact directly with incoming signals. A copper plate is placed behind this layer to prevent signal energy loss. The inner layer is a control circuit board. Positive-intrinsic-negative (PIN) diode is embedded into each RIS element that adjusts the reflection amplitude/phase shift of each element [27]. In the literature, many studies related to RIS-aided wireless communication systems that consider ideal reflection model assume that the phases and amplitudes of unit cells can be modeled as two independent variables. However, in practical systems, this assumption is not applicable, since the reflection

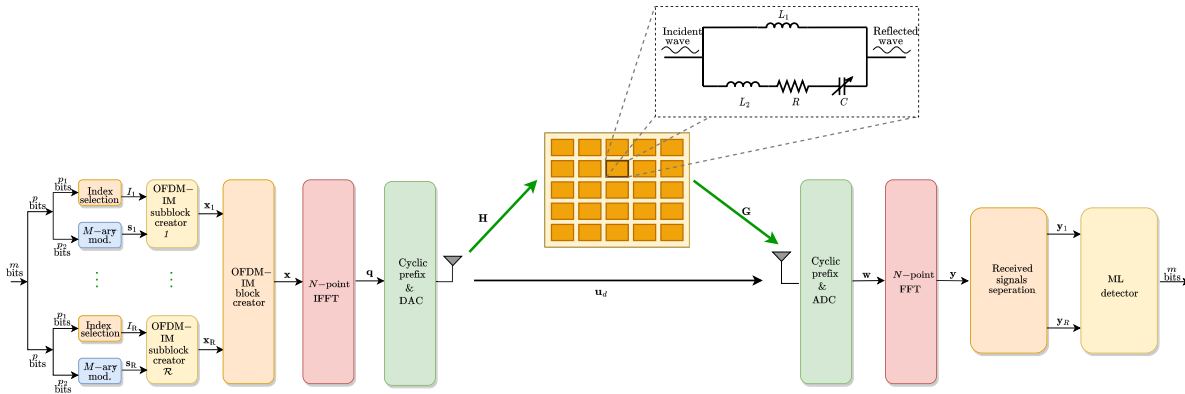


FIGURE 1. RIS-aided OFDM-IM system model.

coefficient of the RIS unit cell depends not only on the parameters of the circuit but also on the frequency of the impinging signal. That means there is an elementary relationship between the phase shift and amplitude of a RIS element. For this aim, to demonstrate the relationship between the amplitude and phase of the reflection coefficient, the response of any reflection element will be modeled equivalently as a parallel resonant circuit, which is illustrated in FIGURE 1. Here, by choosing the appropriate value for capacitance  $C$ , the amplitude and phase shift of the reflecting element can be controlled. The impedance of the reflecting RIS element for a frequency of the incident signal can be denoted as

$$Z(C, f) = \frac{j2\pi fL_1 \left( j2\pi fL_2 + \frac{1}{j2\pi fC} + R \right)}{j2\pi fL_1 + \left( j2\pi fL_2 + \frac{1}{j2\pi fC} + R \right)} \quad (1)$$

where  $C$ ,  $R$ ,  $L_1$  and  $L_2$  stand for equivalent effective capacitance, loss resistance and bottom and top layer inductance of the circuit, respectively. Thus, the RIS reflection coefficient can be written as function of capacitance and frequency,

$$\phi(C, f) = \frac{Z(C, f) - Z_0}{Z(C, f) + Z_0} \quad (2)$$

where  $Z(C, f)$  given in (1) and  $Z_0 = 377\Omega$  denotes free space empedance. The relationship between RIS reflection coefficient and the frequency of the impinging signal can be clearly observed from (2), that means any RIS element can display different responses according to the frequency of the incident signal. It is worth saying that since the metal element of RIS is connected to each other through PIN diode, the electrical characteristics of a RIS element are shown by parallel resonant circuit and the impedance is given by (1). As shown in (2), phase and amplitude of the RIS element depend on the impedance of the RIS element that changes with respect to the frequency. It is noted that the consideration of an accurate model is very critical for the use of RIS solutions for wideband communication systems. The reflection coefficient of the  $m$ -th element of RIS be defined as

$$\phi_m = A_m e^{j\theta_m}, \quad \forall m, \quad (3)$$

where  $\theta_m \in [-\pi, \pi)$  and  $A_m \in [0, 1]$  stand for phase shift and amplitude of the  $m$ -th reflection coefficient  $\phi_m$ , respectively. Therefore, when the analytical model for the relationship between the reflecting coefficient of the RIS element and the frequency of the incident wave developed in [15] is considered for a bandwidth of  $B$ (MHz) and a carrier frequency of  $f_c$ (GHz), corresponding RIS reflection coefficients of the same element at a different frequency of  $f$  obtained as

$$\begin{aligned} A_m(\angle\phi_c, f) &= \frac{\rho_1 \angle\phi_c + \mu_1}{((f/10^9 - \mathcal{G}_1(\angle\phi_c))/0.05)^2 + 4} + 1, \\ \theta_m(\angle\phi_c, f) &= -2 \tan^{-1} \left[ \mathcal{G}_2(\angle\phi_c) \left( f/10^9 - \mathcal{G}_1(\angle\phi_c) \right) \right], \\ \mathcal{G}_1(\angle\phi_c) &= \rho_2 \tan(\angle\phi_c/3) + \rho_3 \sin(\angle\phi_c) + \mu_2, \\ \mathcal{G}_2(\angle\phi_c) &= \rho_4 \angle\phi_c + \mu_3 \end{aligned} \quad (4)$$

where  $\rho_1, \rho_2, \rho_3, \rho_4, \mu_1, \mu_2, \mu_3$  are the parameters whose exact values are given in [15] according to specific circuit implementation. Here,  $\angle\phi_c$  corresponds to the phase shift of RIS element at the carrier frequency of  $f_c$ .  $A_m(\angle\phi_c, f)$  and  $\theta_m(\angle\phi_c, f)$  denote amplitude and phase shift of  $m$ -th RIS element as a functions of  $\angle\phi_c$  and  $f$ , respectively.

In order to better understand the effect of a practical RIS reflection model for wideband signals, in FIGURE 2(a) and FIGURE 2(b) the amplitude and phase shift value of a RIS element with respect to the incident signal's frequency is given, respectively. It can be observed that the given practical RIS model in [15] completely matches with the analytical model of the RIS reflection coefficient. It is worth noting that in FIGURE 2(a) and FIGURE 2(b), while dash lines correspond to the mathematical model of the RIS element given in (2), solid lines belong to the fitted model which is given in (4). Also, it can be clearly seen that amplitude and phase shift values of the RIS unit cells vary with the incident wave's frequency, which is very significant for a wideband signal while optimizing the reflection coefficient of RIS elements. This situation makes necessary to consider the practical RIS model given in (4) for the OFDM-IM communication system.

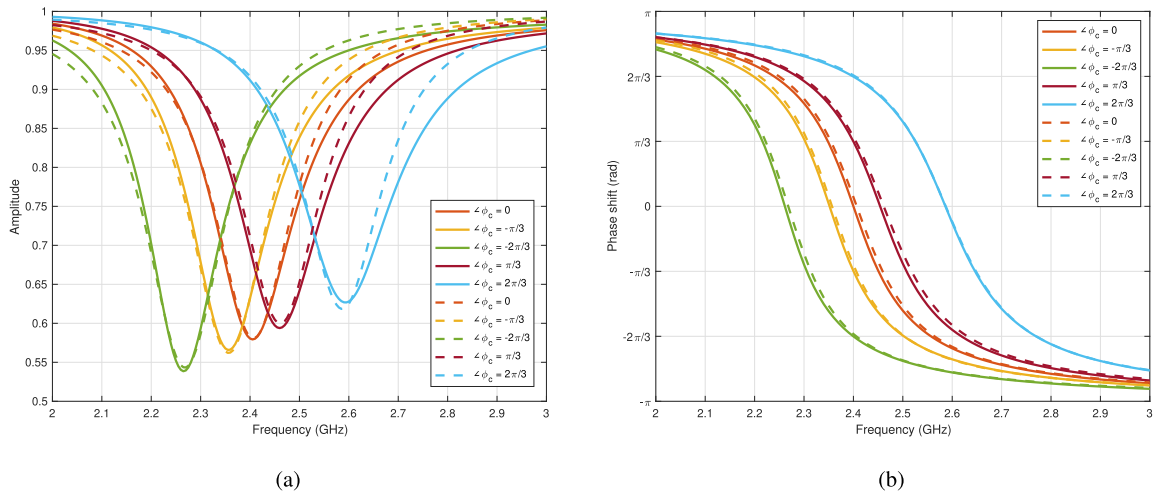


**FIGURE 2.** Variation of (a) Amplitude and (b) Phase shift of RIS reflection coefficient with respect to changing frequency. Solid Line: fitted model, Dash Line: mathematical model.

**B. SYSTEM MODEL**

In this paper, as illustrated FIGURE 1, RIS-aided wideband OFDM-IM system from a single-antenna BS to a single-antenna user with  $N$  subcarriers and  $M$  passive RIS elements is considered. Let  $\mathbf{H} = [\mathbf{h}_1, \dots, \mathbf{h}_N] \in \mathbb{C}^{M \times N}$ ,  $\mathbf{G} = [\mathbf{g}_1, \dots, \mathbf{g}_N] \in \mathbb{C}^{M \times N}$  and  $\mathbf{u}_d \in \mathbb{C}^N$  denote the channel frequency responses (CFR) of BS-RIS direct link, RIS-user link and BS-user direct link, respectively.

In the proposed OFDM-IM system, different from traditional OFDM systems, the total number of subcarriers,  $N$ , is divided into  $R$  subblocks, each of which consists of  $L = N/R$  subcarriers. In each subblock, the first  $p_1 = \lceil \log_2(C(L, k)) \rceil$  bits of the incoming  $p$  bits are used to activate  $k$  subcarriers out of  $L$  ones according to the look-up table in [19], while the last  $p_2 = k \log_2 M$  bits are mapped to  $M$ -ary signal constellation in order to choose data symbols which modulate active subcarriers. After concatenating a set of  $R$  subblocks adjacently, in the frequency domain, the transmitted OFDM-IM symbol can be denoted as  $\mathbf{x} = [x_1, \dots, x_N]^T \in \mathbb{C}^N$ , where the total transmit power can be expressed by  $P_t = \text{Tr}\{\mathbb{E}\{\mathbf{x}^H \mathbf{x}\}\}$ . Then, the communication procedure follows the traditional OFDM transmission, in which the OFDM-IM symbol  $\mathbf{x}$ , is transformed into the time domain via an  $N$ -point inverse fast Fourier transform (IFFT). At the output of IFFT procedure, to the beginning of the symbol, a cyclic prefix (CP) of length  $L_{cp}$  is appended in order to mitigate the inter-symbol-interference. After removing the CP, an  $N$ -point FFT procedure is performed at the receiver side, and for the  $n$ -th subcarrier received signal  $y_n$  is obtained in the frequency domain, which is given as follows

$$y_n = (\mathbf{h}_n^H \Phi_n \mathbf{g}_n + u_{d,n}) x_n + v_n \quad \forall n, \quad (5)$$

where  $\mathbf{h}_n \in \mathbb{C}^M$  and  $\mathbf{g}_n \in \mathbb{C}^M$  are  $n$ -th column of  $\mathbf{H}$  and  $\mathbf{G}$  channel matrices, respectively. Besides,  $u_{d,n}$  is the  $n$ -th element of the direct channel between the BS-user link, and  $v_n \sim \mathcal{CN}(0, \sigma^2)$  is the additive white Gaussian

noise (AWGN) sample with zero mean and variance  $\sigma^2$ .  $\Phi_n = \text{diag}(\phi_n) = \text{diag}([\phi_{n,1}, \dots, \phi_{n,M}]) \in \mathbb{C}^{M \times M}$ . In here,  $|\phi_{n,m}|$  and  $\angle \phi_{n,m}$  corresponds to the amplitude and the phase shift of the  $m$ -th RIS element for the  $n$ -th subcarrier, respectively. In an ideal RIS model, the reflection coefficients of the RIS elements are same for all subcarriers such as  $|\phi_{1,m}| = \dots = |\phi_{N,m}| = 1$ ,  $\angle \phi_{1,m} = \dots = \angle \phi_{N,m}$ ,  $\forall m$ . Nevertheless, this assumption is not practical for wideband communication systems since the RIS reflection coefficients vary with respect to the frequency of the impinging signal as it is demonstrated in FIGURE 2(a) and FIGURE 2(b). Therefore, for the reflection coefficient optimization of RIS-aided OFDM-IM system, we consider the practical RIS model given in (4), i.e.,

$$\begin{aligned} |\phi_{n,m}| &= A_m(\angle \phi_{c,m}, f_n), \\ \angle \phi_{n,m} &= \theta_m(\angle \phi_{c,m}, f_n), \quad \forall n, \forall m \end{aligned} \quad (6)$$

where  $\angle \phi_{c,m}$  represents the phase shift value of  $m$ -th RIS element.  $f_n$  and  $f_c$  correspond to the central frequency of each subcarrier and carrier frequency, respectively which can be described as  $f_n \triangleq f_c + (n - \frac{N+1}{2}) \frac{B}{N}$ . By using the received signal model for OFDM-IM system, which is defined in (5), we will consider the reflection coefficient optimization problem in the next section.

**III. REFLECTION COEFFICIENT OPTIMIZATION FOR OFDM-IM**

In this section, we aim to optimize the reflection coefficients for the proposed OFDM-IM system. In the literature, many studies focus on the optimization of the reflection coefficients for OFDM systems by maximizing the average achievable rate [11], [12], [15], [16], [28]. To the best of our knowledge, the design of reflection coefficients for RIS aided OFDM-IM systems has not yet been addressed. Since some of the subcarriers are empty in OFDM-IM systems, we need to reformulate the reflection coefficient design problem separately from the

**Algorithm 1** Reflection Coefficient Design  $\hat{\phi}_c$  With Discrete Phase Shifts**Require:**  $\mathbf{h}_n, \mathbf{g}_n, u_{d,n}, \mathcal{B}, \mathcal{S}, R$ **Ensure:**  $\hat{\phi}_c$ 

```

1: Assign  $iter = 0$ 
2: Initialize  $\angle\phi_{c,m}^{(iter)}$ ,  $m = 1, \dots, M$  from the set  $\mathcal{B}$ .
3: Initialize  $\angle\phi_{c,m}^{(temp)} = 0$ ,  $m = 1, \dots, M$ .
4: while  $\|\angle\phi_{c,m}^{(iter)} - \angle\phi_{c,m}^{(temp)}\|^2 > \epsilon$  do
5:    $\angle\phi_{c,m}^{(temp)} = \angle\phi_{c,m}^{(iter)}$ 
6:    $iter = iter + 1$ 
7:   for  $m = 1$  to  $M$  do
8:     for  $b = 1$  to  $\mathcal{B}_{max}$  do  $\triangleright \mathcal{B}_{max} = |\mathcal{B}|$ 
9:       Set a value for  $\angle\phi_{c,m}^{(iter)} = \mathcal{B}(b)$ 
10:      for  $n = 1$  to  $N$  do
11:        Set  $|\phi_{n,m}| = A_m(\angle\phi_{c,m}, f_n)$ ,
12:         $\angle\phi_{n,m} = \theta_m(\angle\phi_{c,m}, f_n)$ ,
13:      end for
14:      for  $r = 1$  to  $R$  do
15:        Calculate  $d_{\min}(\tilde{\mathbf{H}}_r)$  with (8).
16:      end for
17:      Calculate AMED,  $d(\tilde{\mathbf{H}})$  by (9).
18:    end for
19:    Obtain  $\angle\phi_{c,m}^{(iter)}$  which has maximum AMED.
20:  end for
21: end while
22:  $\hat{\phi}_c = [\angle\phi_{c,1}, \dots, \angle\phi_{c,M}]$ .

```

maximization of the achievable rate. Therefore, the methods aiming to improve the system performance of OFDM-IM systems have been investigated and it has been seen that most of the designs for the OFDM-IM systems were established to minimize bit error rate (BER) performance. It has been stated that BER is more susceptible to the Euclidean distances of available transmit vectors, especially in high SNR regime [29]. However, the OFDM-IM system can produce superior performance than conventional methods if it is based on the maximization of MED criterion [23], [24], [25], [26], [30]. Since it is challenging to obtain a BER expression for the RIS-aided OFDM-IM system, the reflection coefficient optimization problem is formulated based on the maximization of the MED criterion in order to simplify the design. It is worth saying that in the conventional OFDM-IM system, the BER performances in the different subblocks are same, whereas, when we combine the OFDM-IM system with the practical RIS model which is given in (4), the BER performance will be different in each subblock. Thus, we specify a new optimization objective which is called AMED [24]. Before we define the AMED expression, we first provide the received vectors and their minimum Euclidean distance for the  $r$ -th subblock respectively:

$$\begin{aligned} \mathbf{y}_r &= (\mathbf{H}_r^H \Phi_r \mathbf{G}_r + \mathbf{u}_{d,r}) \mathbf{x}_r + \mathbf{v}_r, \\ &= \tilde{\mathbf{H}}_r^H \mathbf{x}_r + \mathbf{v}_r, \end{aligned} \quad (7)$$

where  $\mathbf{H}_r \in \mathbb{C}^{L \times M}$  and  $\mathbf{G}_r \in \mathbb{C}^{L \times M}$  are the channel matrices of the  $r$ -th subblock of OFDM-IM system. Here  $\tilde{\mathbf{H}} \triangleq \mathbf{H}^H \Phi \mathbf{G} + \mathbf{u}_d$  denote the superimposed channel frequency response (CFR) from the BS to the user by combining the cascaded channel BS/RIS/user and the direct channel from the BS to the user and  $\tilde{\mathbf{H}}_r$  is the superimposed CFR for the  $r$ -th subblock, while  $\mathbf{y}_r \in \mathbb{C}^L$  and  $\mathbf{x}_r \in \mathbb{C}^L$  are the received vector and the transmitted OFDM-IM symbol for the  $r$ -th subblock, respectively. The MED of the received vector for the  $r$ -th subblock is given as:

$$d_{\min}(\tilde{\mathbf{H}}_r) = \min_{\substack{\mathbf{x}_{r,i}, \mathbf{x}_{r,j} \in \mathcal{S} \\ \mathbf{x}_{r,i} \neq \mathbf{x}_{r,j}}} \left\| \tilde{\mathbf{H}}_r (\mathbf{x}_{r,i} - \mathbf{x}_{r,j}) \right\|_2^2 \quad (8)$$

where  $\mathcal{S}$  denotes the set of all possible transmit vectors for each subblock and  $\mathbf{x}_{r,i}$  and  $\mathbf{x}_{r,j}$  are transmit vectors for  $r$ -th subblock from the set of  $\mathcal{S}$ .

Then, AMED among the subblocks can be calculated as

$$\begin{aligned} d(\tilde{\mathbf{H}}) &= \frac{1}{R} \sum_{r=0}^{R-1} d_{\min}(\tilde{\mathbf{H}}_r) \\ &= \frac{1}{R} \sum_{r=0}^{R-1} \min_{\substack{\mathbf{x}_{r,i}, \mathbf{x}_{r,j} \in \mathcal{S} \\ \mathbf{x}_{r,i} \neq \mathbf{x}_{r,j}}} \left\| \tilde{\mathbf{H}}_r (\mathbf{x}_{r,i} - \mathbf{x}_{r,j}) \right\|_2^2 \end{aligned} \quad (9)$$

Then, to optimize the reflection coefficient of the RIS  $\phi_c = [\angle\phi_{c,1}, \dots, \angle\phi_{c,M}]^T$  the following maximization problem is formulated:

$$\begin{aligned} \max_{\phi_c} & d_{\phi_c}(\tilde{\mathbf{H}}) \\ \text{s.t.} & |\phi_{n,m}| = A_m(\angle\phi_{c,m}, f_n), \\ & \angle\phi_{n,m} = \theta_m(\angle\phi_{c,m}, f_n), \\ & \angle\phi_{c,m} \in \mathcal{B}, \end{aligned} \quad (10)$$

where  $d_{\phi_c}(\tilde{\mathbf{H}}) \triangleq \frac{1}{R} \sum_{r=0}^{R-1} d_{\min}(\tilde{\mathbf{H}}_r, \phi_c)$  and  $\tilde{\mathbf{H}}_r, \phi_c$  is superimposed CFR of  $r$ -th subblock corresponding to the preset the RIS reflection coefficient. In the practical model of RIS systems, phase shifts of RIS elements at the center frequency  $f_c$  have discrete values which are regulated with the finite number of bits,  $Q$ .  $\angle\phi_{c,m}$  can be defined as:

$$\angle\phi_{c,m} \in \mathcal{B} \triangleq \left\{ -\pi, (\Delta\phi - \pi), \dots, ((2^Q - 1) \Delta\phi - \pi) \right\}, \quad (11)$$

where  $\Delta\phi = 2\pi/2^Q$ . Because of the fact that we have discrete phase values for RIS elements, we propose an exhaustive search algorithm in order to obtain an optimal phase shift for the center frequency of one RIS unit cell by using previous phase shifts of other RIS elements. Explicitly, to obtain optimal  $\angle\phi_{c,m}$ , all possible phase shift values from the set  $\mathcal{B}$  are checked and the reflection coefficient values for different subcarriers according to the practical reflection model as given in (4) are calculated. After that, the best reflection coefficient value  $\angle\phi_{c,m}$  is selected from the set  $\mathcal{B}$ , which maximizes the AMED,  $d_{\phi_c}(\tilde{\mathbf{H}})$ . As a result, the design procedure of the reflection coefficient optimization for the OFDM-IM system with discrete phase shift is summarized in Algorithm 1.

TABLE 1. Simulation parameters.

Modulation Type	BPSK
# of subcarriers	$N = 64$
# of subblocks in each OFDM-IM symbol	$R = 16$
# of available subcarriers in each subblock	$L = 4$
# of active subcarriers in each subblock	$k = 2$
# of bits carrier by a symbol	$m = Rp$
CP length	$L_{cp} = 16$
Bit energy	$E_b = (N + L_{cp})/m$
Carrier frequency	$f_c = 2.4$ GHz
# of RIS elements	$M = 64$
# of bits for discrete phase shifts	$Q = 3$
# of channel taps for all channels	$L_1 = L_2 = L_d = 8$
Bandwidth of channel	$B = 100$ MHz
Noise power	$\sigma^2 = -80$ dBm

IV. SIMULATION RESULTS

In this section, we provide extensive computer simulation results in order to investigate the BER performance of the proposed algorithm for RIS-aided OFDM-IM system. The simulation parameters are listed in Table 1. A frequency selective Rayleigh fading channel with  $L_1 = L_2 = L_d = 8$  exponentially decaying taps are considered for BS-RIS, RIS-user and BS-user direct links, respectively. While the distances between the BS-RIS and the BS-user are adjusted as  $d_{BR} = d_{BU} = 50$  m and the distance between RIS-user is designated as  $d_{RU} = 2$  m. The path loss with respect to the selected distance  $d$  is modeled by  $PL = C_0(d/d_0)^\xi$  where  $C_0 = 30$  dB is signal attenuation at a reference distance  $d_0 = 1$  m and  $\xi$  is the path loss exponent parameter. Path loss exponent values for the BS-RIS, the RIS-user and the BS-user channels are adjusted as  $\xi_{BR} = 2.5$ ,  $\xi_{RU} = 2.8$  and  $\xi_{BU} = 3.5$ , respectively.

First, we examine the convergence of the proposed exhaustive search-based reflection design algorithm by plotting the AMED according to the number of iterations for  $M = 64$  and 128 in FIGURE 3 and FIGURE 4, respectively. In here,  $Q$  denotes the number of bit resolution whose detail is given in (11). Simulation results show that when the bit resolution,  $Q$ , increases, the AMED value increases for both  $M = 64$  and 128 RIS elements. As it is expected, when the number of bit resolutions becomes larger, the gap between the maximum AMED values decreases. Besides, comparing FIGURE 3 and FIGURE 4 in terms of the AMED values, it is clearly seen that growing the number of RIS elements can effectively enhance the AMED.

In FIGURE 5, we illustrate the AMED value with respect to the number of RIS elements for different bit resolutions. FIGURE 5 demonstrates compatible behavior with the convergence results of AMED value which are shown in FIGURE 3 and FIGURE 4. Similarly, the gap between AMED values decreases by the increasing number of bit resolutions.

Next, in FIGURE 6, we investigate the BER performances of OFDM and OFDM-IM systems with the practical model given in (4). In this figure, reflection coefficient values are optimized according to the average achievable rate criteria

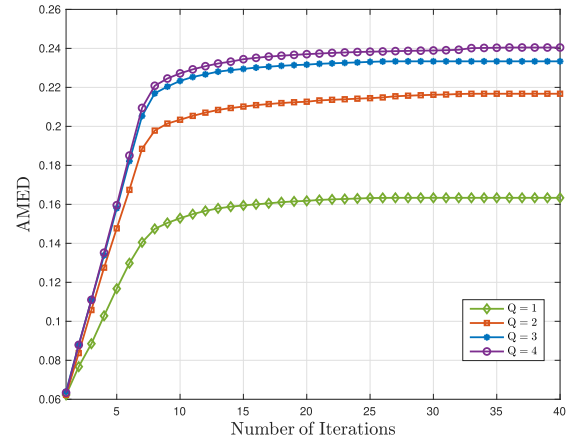


FIGURE 3. AMED versus number of iterations ( $N = 64, M = 64$ ).

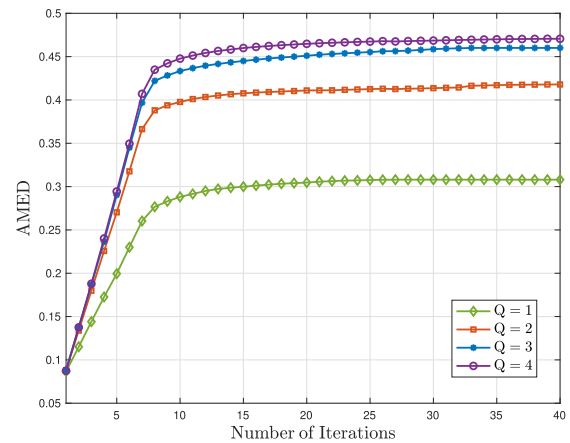


FIGURE 4. AMED versus number of iterations ( $N = 64, M = 128$ ).

for both OFDM and OFDM-IM systems. For the “ideal model” case, reflection coefficient values are designed by the ideal RIS model, however, testified with the practical RIS model as in [16]. It is clearly seen that especially for the wideband communication system, the practical RIS model provides noticeably better BER performance according to the ideal RIS model. When the performances of OFDM and OFDM-IM systems are compared, the observed results demonstrate similar behaviors with and without RIS cases in which the OFDM-IM shows a better performance than the OFDM system in high SNR region.

In FIGURE 7, we illustrate the BER performances of the RIS-aided OFDM-IM system with the average achievable rate criterion and the proposed AMED criterion, at several values of the RIS element size,  $M$ . Obviously, it can be seen that the proposed model provides a 3 dB  $E_b/N_0$  gain over the average achievable rate-based practical model at a BER =  $10^{-5}$  of  $M = 64$ . The reason behind this can be explained as in the OFDM-IM system, where some of the subcarriers are empty and the average achievable rate criterion does not provide optimal reflection coefficient values for the RIS elements. Instead of this method, when we design the optimization problem based on the maximization of AMED

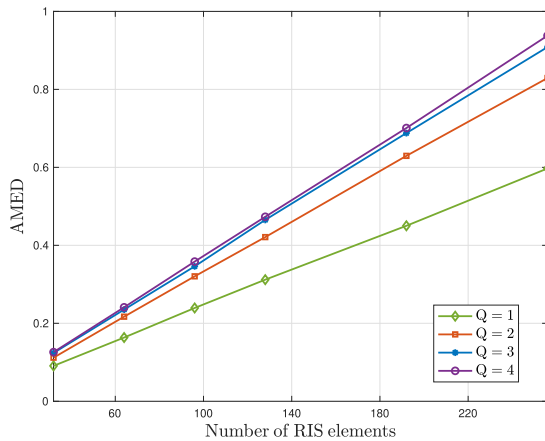


FIGURE 5. AMED versus number of RIS elements ( $N = 64$ ).

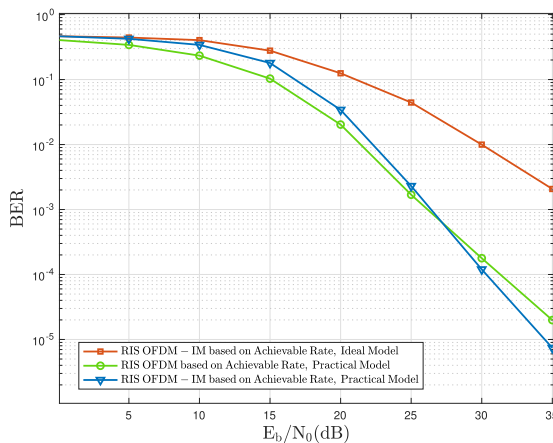


FIGURE 6. BER performance versus  $E_b/N_0$  (dB) ( $N = 64, M = 64, Q = 3$ ).

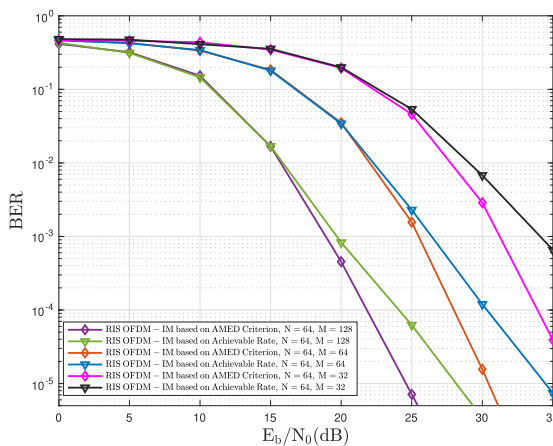


FIGURE 7. BER performance versus  $E_b/N_0$  (dB) with proposed model ( $N = 64, Q = 3$ ).

and obtain the optimal reflection coefficient values according to this criterion, this results in a better BER performance. Similarly, for  $M = 128$ , our proposed model has higher performance than the achievable rate criterion. As expected, the BER performances of both schemes, the achievable rate and the AMED, significantly improve by increasing the  $M$  value from 32 to 128.

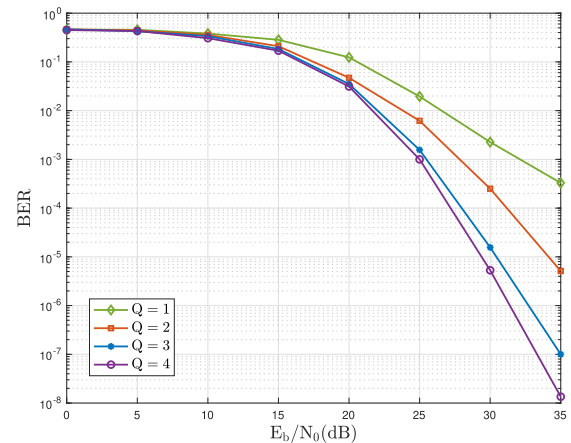


FIGURE 8. BER performance versus  $E_b/N_0$  (dB) with proposed model for different bit resolutions ( $N = 64, M = 64$ ).

Finally, in order to illustrate the relation between the AMED value and the BER performance, we investigate the BER performance of the RIS-aided OFDM-IM system with the proposed model for different bit resolutions from  $Q = 1$  to  $Q = 4$  in FIGURE 8. It can be seen that there is a harmonious relationship between the graph of change in AMED value according to different bit resolutions given in FIGURE 3 and the BER performance of different bit resolutions in this figure. Similar to FIGURE 3, as the bit resolution value increases, the speed of the performance improvement of BER decreases. This relation demonstrates the advantage of reflection coefficient design optimization of OFDM-IM system by considering maximization of AMED value.

## V. CONCLUSION

In this study, we have primarily demonstrated the importance of the practical RIS reflection model, especially for a wide-band communication system utilizing OFDM-based waveforms. Based on the practical RIS model, we have designed the reflection coefficient values for OFDM and OFDM-IM systems by maximizing the average achievable rate. Then, in order to further enhance the BER performance of the RIS-aided OFDM-IM system, we have reformulated the optimization problem for the RIS reflection coefficient with respect to the AMED criterion. Simulation results have shown that the proposed algorithm achieves better BER performance for the OFDM-IM system concerning the existing optimization algorithm based on maximizing the average achievable rate of all subcarriers. As a future work, we will focus on power allocation algorithm for RIS-aided OFDM-IM system by jointly designing the RIS reflection coefficient and transmit beamformer to improve the performance of the system further.

## REFERENCES

[1] E. Basar, M. Di Renzo, J. De Rosny, M. Debbah, M. Alouini, and R. Zhang, "Wireless communications through reconfigurable intelligent surfaces," *IEEE Access*, vol. 7, pp. 116753–116773, 2019.

- [2] E. Basar, "Reconfigurable intelligent surface-based index modulation: A new beyond MIMO paradigm for 6G," *IEEE Trans. Commun.*, vol. 68, no. 5, pp. 3187–3196, May 2020.
- [3] E. Basar, "Transmission through large intelligent surfaces: A new frontier in wireless communications," in *Proc. Eur. Conf. Netw. Commun. (EuCNC)*, Jun. 2019, pp. 112–117.
- [4] W. Cai, R. Liu, M. Li, Y. Liu, Q. Wu, and Q. Liu, "IRS-assisted multi-cell multiband systems: Practical reflection model and joint beamforming design," *IEEE Trans. Commun.*, vol. 70, no. 6, pp. 3897–3911, Jun. 2022.
- [5] C. Huang, A. Zappone, G. C. Alexandropoulos, M. Debbah, and C. Yuen, "Reconfigurable intelligent surfaces for energy efficiency in wireless communication," *IEEE Trans. Wireless Commun.*, vol. 18, no. 8, pp. 4157–4170, Aug. 2019.
- [6] P. Wang, J. Fang, L. Dai, and H. Li, "Joint transceiver and large intelligent surface design for massive MIMO mmWave systems," *IEEE Trans. Wireless Commun.*, vol. 20, no. 2, pp. 1052–1064, Feb. 2021.
- [7] Z. Li, M. Hua, Q. Wang, and Q. Song, "Weighted sum-rate maximization for multi-IRS aided cooperative transmission," *IEEE Wireless Commun. Lett.*, vol. 9, no. 10, pp. 1620–1624, Oct. 2020.
- [8] S. Zhou, W. Xu, K. Wang, M. Di Renzo, and M.-S. Alouini, "Spectral and energy efficiency of IRS-assisted MISO communication with hardware impairments," *IEEE Wireless Commun. Lett.*, vol. 9, no. 9, pp. 1366–1369, Sep. 2020.
- [9] Q. Wu and R. Zhang, "Intelligent reflecting surface enhanced wireless network via joint active and passive beamforming," *IEEE Trans. Wireless Commun.*, vol. 18, no. 11, pp. 5394–5409, Nov. 2019.
- [10] X. Yu, D. Xu, and R. Schober, "MISO wireless communication systems via intelligent reflecting surfaces," in *Proc. IEEE/CIC Int. Conf. Commun. China (ICCC)*, Aug. 2019, pp. 735–740.
- [11] Y. Yang, B. Zheng, S. Zhang, and R. Zhang, "Intelligent reflecting surface meets OFDM: Protocol design and rate maximization," *IEEE Trans. Commun.*, vol. 68, no. 7, pp. 4522–4535, Jul. 2020.
- [12] B. Zheng and R. Zhang, "Intelligent reflecting surface-enhanced OFDM: Channel estimation and reflection optimization," *IEEE Wireless Commun. Lett.*, vol. 9, no. 4, pp. 518–522, Apr. 2019.
- [13] H. Li, R. Liu, M. Li, Q. Liu, and X. Li, "IRS-enhanced wideband MU-MISO-OFDM communication systems," in *Proc. IEEE Wireless Commun. Netw. Conf. (WCNC)*, May 2020, pp. 1–6.
- [14] S. Abeywickrama, R. Zhang, Q. Wu, and C. Yuen, "Intelligent reflecting surface: Practical phase shift model and beamforming optimization," *IEEE Trans. Commun.*, vol. 68, no. 9, pp. 5849–5863, Sep. 2020.
- [15] W. Cai, H. Li, M. Li, and Q. Liu, "Practical modeling and beamforming for intelligent reflecting surface aided wideband systems," *IEEE Commun. Lett.*, vol. 24, no. 7, pp. 1568–1571, Jul. 2020.
- [16] H. Li, W. Cai, Y. Liu, M. Li, Q. Liu, and Q. Wu, "Intelligent reflecting surface enhanced wideband MIMO-OFDM communications: From practical model to reflection optimization," *IEEE Trans. Commun.*, vol. 69, no. 7, pp. 4807–4820, Jul. 2021.
- [17] E. Başar, "Index modulation techniques for 5G wireless networks," *IEEE Commun. Mag.*, vol. 54, no. 7, pp. 168–175, Jul. 2016.
- [18] R. Y. Mesleh, H. Haas, S. Sinanovic, C. W. Ahn, and S. Yun, "Spatial modulation," *IEEE Trans. Veh. Technol.*, vol. 57, no. 4, pp. 2228–2241, Jul. 2008.
- [19] E. Başar, U. Aygözü, E. Panayırçı, and H. V. Poor, "Orthogonal frequency division multiplexing with index modulation," *IEEE Trans. Signal Process.*, vol. 61, no. 22, pp. 5536–5549, Nov. 2013.
- [20] P. Yang, Y. L. Guan, Y. Xiao, M. D. Renzo, S. Li, and L. Hanzo, "Transmit precoded spatial modulation: Maximizing the minimum Euclidean distance versus minimizing the bit error ratio," *IEEE Trans. Wireless Commun.*, vol. 15, no. 3, pp. 2054–2068, Mar. 2016.
- [21] S. Guo, H. Zhang, P. Zhang, S. Dang, C. Liang, and M.-S. Alouini, "Signal shaping for generalized spatial modulation and generalized quadrature spatial modulation," *IEEE Trans. Wireless Commun.*, vol. 18, no. 8, pp. 4047–4059, Aug. 2019.
- [22] J. Luo, S. Wang, and F. Wang, "Joint transmitter-receiver spatial modulation design via minimum Euclidean distance maximization," *IEEE J. Sel. Areas Commun.*, vol. 37, no. 9, pp. 1986–2000, Sep. 2019.
- [23] J. Zheng, "Adaptive index modulation for parallel Gaussian channels with finite alphabet inputs," *IEEE Trans. Veh. Technol.*, vol. 65, no. 8, pp. 6821–6827, Aug. 2016.
- [24] Q. Ma, Y. Xiao, L. Dan, P. Yang, L. Peng, and S. Li, "Subcarrier allocation for OFDM with index modulation," *IEEE Commun. Lett.*, vol. 20, no. 7, pp. 1469–1472, Jul. 2016.
- [25] X. Liu, L. Dan, Q. Ma, Y. Xiao, and X. He, "Profile-based power allocation in OFDM with index modulation," in *Proc. IEEE 85th Veh. Technol. Conf. (VTC Spring)*, Jun. 2017, pp. 1–5.
- [26] N. Ishikawa, S. Sugiura, and L. Hanzo, "Subcarrier-index modulation aided OFDM-will it work?" *IEEE Access*, vol. 4, pp. 2580–2593, 2016.
- [27] Q. Wu and R. Zhang, "Towards smart and reconfigurable environment: Intelligent reflecting surface aided wireless network," *IEEE Commun. Mag.*, vol. 58, no. 1, pp. 106–112, Jan. 2019.
- [28] S. Lin, B. Zheng, G. C. Alexandropoulos, M. Wen, and F. Chen, "Progressive channel estimation and passive beamforming for RIS-assisted OFDM systems," in *Proc. IEEE Global Commun. Conf. (GLOBECOM)*, Taiwan, Dec. 2020, pp. 1–6.
- [29] S. Guo, H. Zhang, S. Jin, and P. Zhang, "Spatial modulation via 3-D mapping," *IEEE Commun. Lett.*, vol. 20, no. 6, pp. 1096–1099, Jun. 2016.
- [30] Y. Xiao, S. Wang, L. Dan, X. Lei, P. Yang, and W. Xiang, "OFDM with interleaved subcarrier-index modulation," *IEEE Commun. Lett.*, vol. 18, no. 8, pp. 1447–1450, Aug. 2014.



**ELVAN KUZUCU HIDIR** received the B.S. and M.S. degrees (Hons.) in electrical and electronics engineering from Bilkent University, Turkey, in 2015 and 2017, respectively. She is currently pursuing the Ph.D. degree with Istanbul Technical University. She is also a Research and Teaching Assistant with Istanbul Technical University. Her current research interests include OFDM, index modulation, and intelligent surfaces.



**ERTUGRUL BASAR** (Fellow, IEEE) received the Ph.D. degree from Istanbul Technical University, in 2013.

He is currently an Associate Professor with the Department of Electrical and Electronics Engineering, Koç University, Istanbul, Turkey, and the Director of the Communications Research and Innovation Laboratory (CoreLab). He was a Mercator Fellow at Ruhr University Bochum, Germany, in 2022, and a Visiting Research Collaborator at Princeton University, USA, from 2011 to 2012. His primary research interests include beyond 5G and 6G wireless networks, communication theory and systems, reconfigurable intelligent surfaces, index modulation, waveform design, and signal processing for communications. He is a Young Member of Turkish Academy of Sciences, in 2017. He served as the Editor/Senior Editor for many journals, including *IEEE COMMUNICATIONS LETTERS*, from 2016 to 2022, *IEEE TRANSACTIONS ON COMMUNICATIONS*, from 2018 to 2022, *Physical Communication*, from 2017 to 2020, and *IEEE ACCESS*, from 2016 to 2018. Currently, he is the Editor of *Frontiers in Communications and Networks*.



**HAKAN ALI CIRPAN** (Senior Member, IEEE) received the B.Sc. degree in electrical engineering from Uludağ University, Bursa, Turkey, in 1989, the M.Sc. degree in electrical engineering from Istanbul University, Istanbul, Turkey, in 1992, and the Ph.D. degree in electrical engineering from the Stevens Institute of Technology, Hoboken, NJ, USA, in 1997. From 1995 to 1997, he was a Research Assistant with the Stevens Institute of Technology, working on signal processing algorithms for wireless communication systems. In 1997, he joined the Department of Electrical and Electronics Engineering, Istanbul University. In 2010, he joined the Department of Electronics and Communication Engineering, Istanbul Technical University. His current research interests include machine learning, signal processing, and communication concepts with specific attention to channel estimation, and equalization algorithms for future wireless systems.